

Catalyzed growth model of carbon nanotubes by microwave plasma chemical vapor deposition using CH₄ and CO₂ gas mixtures

Mi Chen^{a,*}, Chieng-Ming Chen^b, Horng-Show Koo^a, Chia-Fu Chen^b

^aDepartment of Chemical Engineering, Minghsin University of Science and Technology Hsinfong, Hsinchu 304, Taiwan, ROC

^bDepartment of Materials Science and Engineering, National Chiao-Tung University, Hsinchu 30049, Taiwan, ROC

Abstract

Catalyst growth carbon nanotubes (CNTs) have been synthesized successfully by microwave plasma chemical vapor deposition using CH₄–CO₂ gas sources, and Fe, Ti, Fe/Ti as catalysts. Significant difference of morphology in the carbon deposition was observed between Fe and Ti catalyst. By adjusting growth parameters of CH₄ to CO₂, a high yield of vertically aligned CNTs can be found in an Fe-deposited substrate. Ti is shown to be not suitable as a catalyst in CNT production. In the present work, we investigated the effect of H₂ plasma pretreatment on the CNT growth from the viewpoint of catalyst morphology, using Fe as the catalyst. After the H₂ pretreatment, significant catalyst particle sintering was observed and resulted in a broad size distribution of catalyst particles. The diameter of CNTs was governed by the catalyst particle size. The diameter of CNTs thus increased as the H₂ plasma pretreated time increased. The CNT diameters were distributed in the range approximately 10–20 nm when Fe-deposited substrate was not pretreated. However, the diameter of CNTs increased from 30 to 300 nm when Fe-deposited substrate was pretreated from 1 to 15 min. The CNT growth model in catalysts, as a function of a gas environment of CH₄–CO₂ gas mixture, was investigated.

© 2003 Elsevier Science B.V. All rights reserved.

Keywords: Carbon; Catalytic process; Plasma; CVD

1. Introduction

Microwave plasma chemical vapor deposition (MPCVD) has been widely used for the growth of carbon nanotubes (CNTs) and diamond film in H₂ and CH₄, H₂ and C₂H₂. Since CNTs were discovered by Iijima [1], many kinds of synthetic techniques have been developed, such as arc discharge, laser ablation, pyrolysis, plasma-enhanced chemical vapor deposition, thermal chemical vapor deposition [2–7]. Some groups emphasized the control of CNT orientation and synthesized well-aligned CNTs by chemical vapor deposition for various catalysts, gas sources and substrates. Dai et al. [8] and Fonseca et al. [9] have studied the use of Fe, Mo, Co, Ni as catalyst particles particularly on Si- and Al-based substrates. The catalyst, reaction temperature and reaction gas play important roles for controlling growth quality of CNTs. Larger-size catalyst

particles with low density and broad diameter are formed at higher temperatures [10]. Rodriguez [11] and Jose-Yacaman et al. [12] have showed that the diameter of tubes was controlled by the metal catalyst particles, which activate CNT growth. Kukovitsky et al. [13] investigated the correlation between metal catalyst particle size and CNT growth. Some groups reported pretreatments as a means of varying and controlling the diameter of CNT and investigated the effect of metal and the mass production methods [14–16].

In our previous studies, MPCVD was successfully used to synthesize multi-walled CNTs by carbon oxide and methane gas mixtures [17]. We found that by substituting carbon oxide for hydrogen in CH₄–CO₂ gas mixture, a high yield vertically aligned multi-walled CNTs could be synthesized at temperatures below 330 °C [18]. We also have investigated the correction between temperature and diameter of CNTs [19]. The diameter of CNTs is influenced by the original catalyst-deposited size at low temperatures. Even at low temperatures, a high yield of CNTs with a high emission current density and small diameter was obtained.

*Corresponding author. Tel.: +886-3-5712121x55346; fax: +886-3-5724727.

E-mail address: chenmi@must.edu.tw (M. Chen).

Table 1
The metal catalyst component

Catalyst	Ti (%)	Fe (%)	Carbon component	Quality
1	100	0	Carbon nanocones	Poor
2	0	100	CNTs	Good
3	50	50	A graphite sheets, CNTs	Fair

In the present work, the effect of various catalysts on CNT growth was studied. The CNTs were deposited from CH₄ and CO₂ gas mixtures by MPCVD process using Fe, Fe/Ti, Ti catalyst, respectively. We investigated the H₂ plasma pretreatment effect on Fe-catalyst morphology and the diameter of CNTs is controlled by the metal catalyst particles. Then, a CNT growth model in catalysts and gas environment of CH₄–CO₂ gas mixture was investigated.

2. Experimental

2.1. The effect of various catalysts on CNT growth

The metal catalyst nanoparticles were deposited on n-type Si(1 0 0) wafer by electron-gun metal evaporation of 10 nm. All metal components are listed in Table 1. The experiments were carried out in a MPCVD reactor. The 20×20 mm² deposited metal-catalyst substrate was pretreated using hydrogen gas with the flow rate of 200 sccm. The microwave power was maintained at 300 W and the total pressure at 15 Torr.

2.2. Effects of H₂ plasma pretreated on Fe-catalyst morphology

The Fe-catalyst nanoparticles were deposited on n-type Si (1 0 0) wafer by sputtering method. The thickness of Fe catalyst was 10 nm. The experiments were carried out in an MPCVD reactor. The 20×20 mm² deposited metal-catalyst substrate was pretreated using hydrogen gas with a flow rate of 200 sccm. The H₂-pretreated time was adjusted from 0 to 15 min. The microwave power was maintained at 400 W and the total pressure at 15 Torr. After the H₂ plasma pretreatment, part of the substrate was cut and an atomic force microscope (AFM) was used to examine the morphology of the Fe catalyst. The remaining part of the H₂-pretreated substrate was reloaded in MPCVD and a

mixture of CH₄ and CO₂ was used as a source gas. The gas flow rates of CH₄ and CO₂ were set at 30 sccm, and DC bias was set at –200 V and was performed to align the CNTs. The deposition conditions are summarized in Table 2.

After deposition, a scanning electron microscope (Hitachi S-4700I) was used to examine the morphology of vertically aligned CNTs. A high-resolution transmission electron microscope (Philips Tecnai-20) was then used to investigate the microstructure of CNTs.

3. Results and discussion

3.1. Effects of various catalysts on CNT growth

Table 1 shows various catalysts for the growth reaction of CNTs. The effect of each catalyst was investigated by keeping power at 300 W and total gas pressure at 15 Torr, while at constant CH₄ and CO₂ flow rate of 30 sccm. The quality of samples is quite good with Fe-deposited substrate, but the vertically aligned carbon nanocones are best formed in Ti-deposited substrate. Vertically aligned CNTs can be obtained but granular ball-like graphite and sheet-like amorphous carbon also appeared on the substrate. The yield of CNTs was less than 20%.

Fig. 1 shows the morphology of carbon deposited using different metal catalysts. Fig. 1a shows the SEM image of CNTs. It can be seen that the CNTs, which were grown on Fe-deposited substrate, are well aligned. Fig. 1b shows the SEM image of the carbon nanocones that were grown on the Ti-deposited substrate, with a negligible amount found. Ti is thus not suitable as a catalyst in CNT production. The Fe/Ti-deposited substrate could be used to grow CNTs but the yield was low. It is likely that if the experimental conditions were optimized, the yield of CNTs can be improved. However, the yield and quality of CNTs strongly depend on the preparation conditions.

3.2. Effects of H₂ plasma pretreated on Fe-catalyst morphology

Fig. 2 shows the typical AFM morphologies of the catalyst particles obtained by the H₂ plasma pretreatment. Fig. 2a shows the microstructure of catalyst surface film before the H₂ plasma pretreatment of the

Table 2
Experimental condition for H₂ plasma pretreatment

No.	H ₂ plasma pretreatment time (min)	CH ₄ /CO ₂ (sccm)	Microwave power (W)	Pressure (Torr)	Deposition time (min)	DC bias (V)
A1	0	30/30	300	15	20	–200
A2	3					
A3	7					
A4	15					

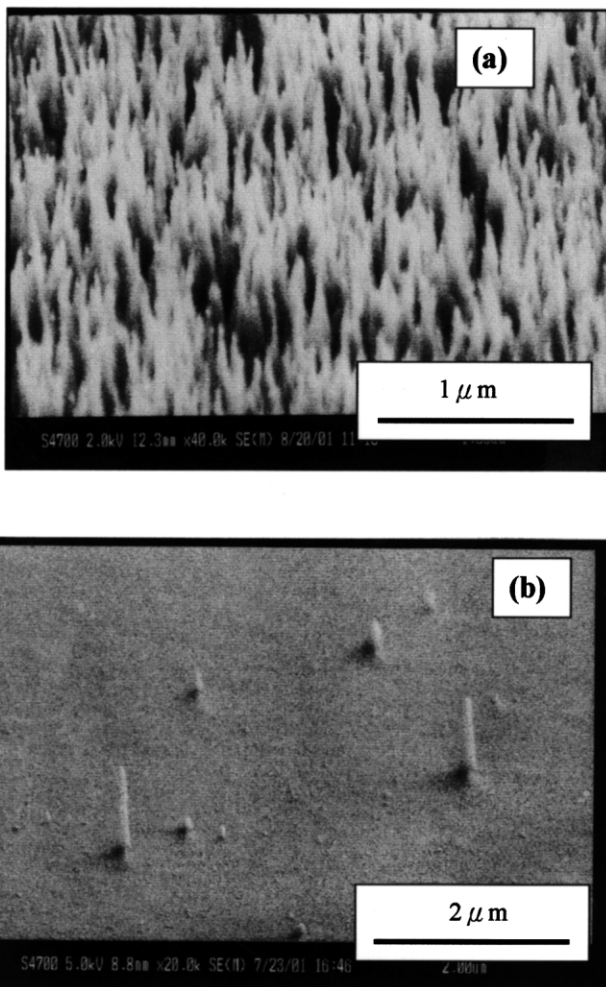


Fig. 1. The morphology of carbon deposited using different metal catalysts. (a) SEM image of CNTs that were grown on the Fe-deposited substrate. (b) SEM image of the carbon nanocones that were grown on the Ti-deposited substrate.

sample. It indicates that Fe particles might be covered with oxide and the surface of particle is not smooth. Fig. 2b shows the Fe-deposited catalyst surface with H_2 plasma pretreated for 3 min. It can be seen that the particle surface becomes smoother and agglomerated due to catalyst sintering. Fe particles stuck together after H_2 plasma pretreatment, leading to a broad size distribution. The Fe particle changed from an approximately spherical to elliptic shape. Fig. 2c and d are the SEM images taken on the Fe-deposited catalyst surface of samples A3 and A4 pretreated with H_2 plasma for 7 min vs. 15 min. Fig. 2c shows that the Fe-catalyst particles on the substrate have become agglomerated. The catalyst particles become longer and more crowded than that for sample A2, and clearly uniform in width. Fig. 2d shows that the particles sintered together were all longer than 200 nm and wider than A3. Hence, the sintering trends of the Fe particle catalytic nanoparticle,

due to the increased H_2 plasma pretreatment time, can be observed.

3.3. Effect of H_2 plasma pretreatment on CNT growth

Fig. 3 shows typical SEM morphology image of vertically aligned CNT growth on an Fe-deposited substrate. Fig. 3a shows SEM image without H_2 plasma pretreatment. It shows the high density and aligned CNTs with diameter approximately 10–20 nm. Further identification of the diameter of CNTs still relies on the observation of high-resolution transmission electron microscopy (HRTEM).

Fig. 3b with H_2 plasma pretreatment for 3 min shows CNTs with diameter of approximately 25–35 nm without 100% vertically aligned as in Fig. 3a. Fig. 3c with H_2 plasma pretreatment for 7 min shows that the size of non-uniform CNTs is of a diameter distributed in the range of approximately 40–90 nm.

Fig. 3d shows SEM image pretreated with H_2 plasma for 15 min. It indicates that the CNTs also are not of uniform size. The diameter is distributed in the range of some 100–200 nm. The Fe particles encapsulated on the tip of CNTs are shown by white arrow in Fig. 3d. The catalyst particle size is clearly larger than the diameter of CNTs.

The relationship between the diameter of CNTs and the H_2 pretreatment time is plotted in Fig. 4. It is illustrated that the diameter of CNTs rose with increased H_2 pretreatment time. After the H_2 plasma pretreatment, the shape and size of Fe particle clearly change. The results prove that the size of catalyst always determines the diameter of CNTs in chemical vapor deposition growth, concluded already by Choi et al. [20].

3.4. HRTEM morphology images of CNTs

Further identification and analysis of CNT growth mechanism still rely on the observation and studies of HRTEM.

Fig. 5 is the HRTEM image for the multi-walled structure of sample A1 and exhibits the Fe particle encapsulated tip with the diameter of ~ 6 nm as shown by white arrow a. The diameter of CNTs is approximately 18 nm and the thickness of CNT wall is approximately 5 nm. A hollow tube with 3-nm diameter and next to a compartment layer is indicated by white arrow b. Arrow c shows a compartment connection with the walls. The Fe particle is of approximately spherical shape. The Fe particle that takes part in various reaction paths of decomposition, diffusion, growth and deposition finally results in the growth of vertical CNTs.

Fig. 6 is the HRTEM image for the multi-walled structure of sample A2. It exhibits the Fe particle encapsulated tip with the diameter of approximately 30 nm, as shown by white arrow. The Fe particle has

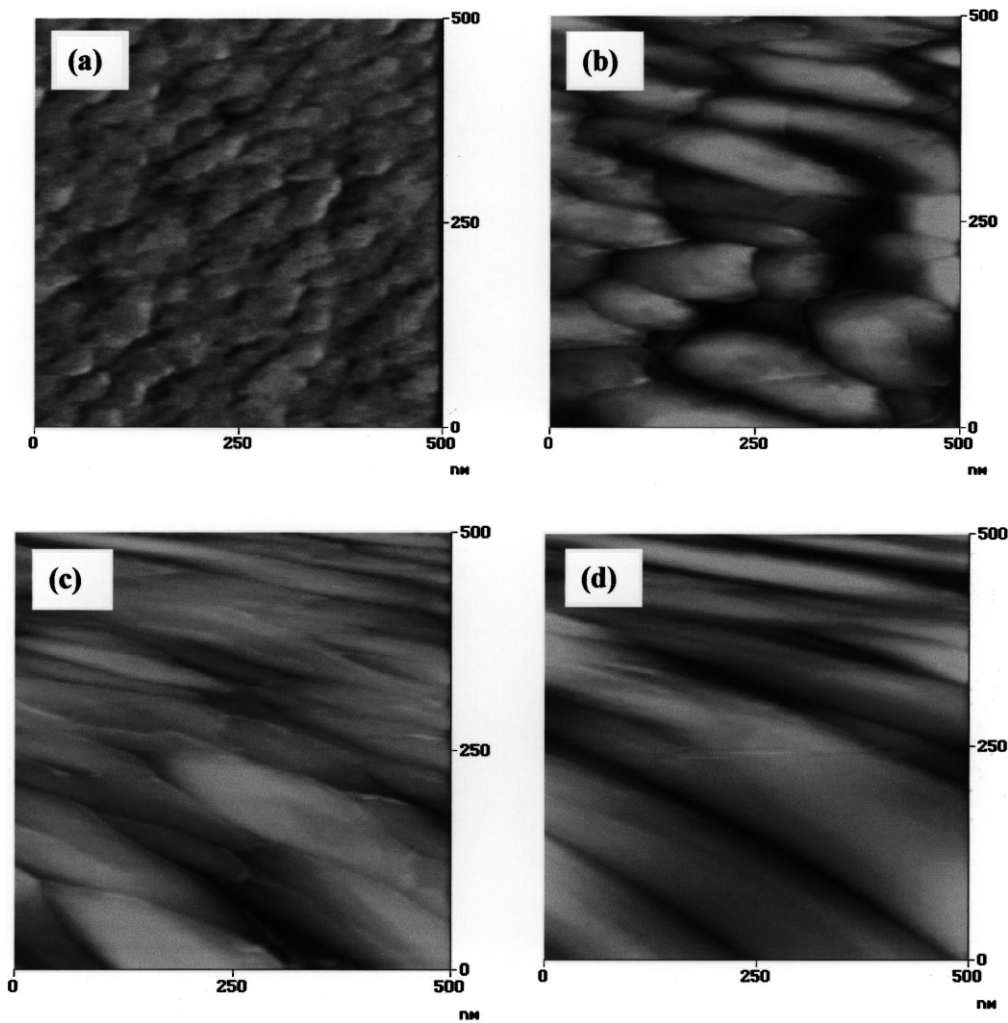


Fig. 2. AFM image with the H_2 plasma pretreatment. (a) Catalyst surface film before H_2 plasma pretreatment of sample. (b) Pretreated with H_2 plasma for 3 min. (c) Pretreated with H_2 plasma for 7 min. (d) Pretreated with H_2 plasma for 15 min.

changed from approximately spherical to the almost elliptic shape. The diameter of CNTs is approximately 30 nm and the thickness of CNT wall is approximately 5 nm. The diameter of Fe-catalyst particle is similar to the diameter of CNTs. Thus, the CNTs grow along the grain of Fe particle, following the trend that the diameter of CNTs is determined by the Fe grain size. The H_2 plasma pretreatment causes the sintering of the Fe particle catalytic nanoparticles, resulting in a cluster of CNTs and a blunter morphology.

3.5. Growth model of carbon nanotubes

Many various growth mechanisms have been illustrated [21–23]; reaction sequences of deposition, adsorption, decomposition, diffusion, growth and deposition vary according to the reaction conditions and species during plasma processing.

A growth model of CNT growth model is speculated in the following text.

Fig. 7 shows the schematic diagram of the growth model of multi-walled CNTs. The CNT growth on Fe particle occurs by the following five steps:

(a) Carbon is disassociated from the CH_4-CO_2 source gases, and deposited toward the surface of Fe particle, where a physical absorption of carbon atoms occurs.

(b) After carbon absorption, a saturated carbon film is formed from the continuous decomposition of source gas and it encapsulated the metal catalyst.

(c) The catalyst and substrate surfaces were saturated with carbon layers, and Fe catalyst was pushed upward due to the diffusion and osmotic pressure, depositing carbon into the graphite structure below the Fe catalyst. When carbon encapsulated Fe particles move quickly upward by continuous osmotic pressure, a core is formed below Fe-catalyst particles because the carbon source is

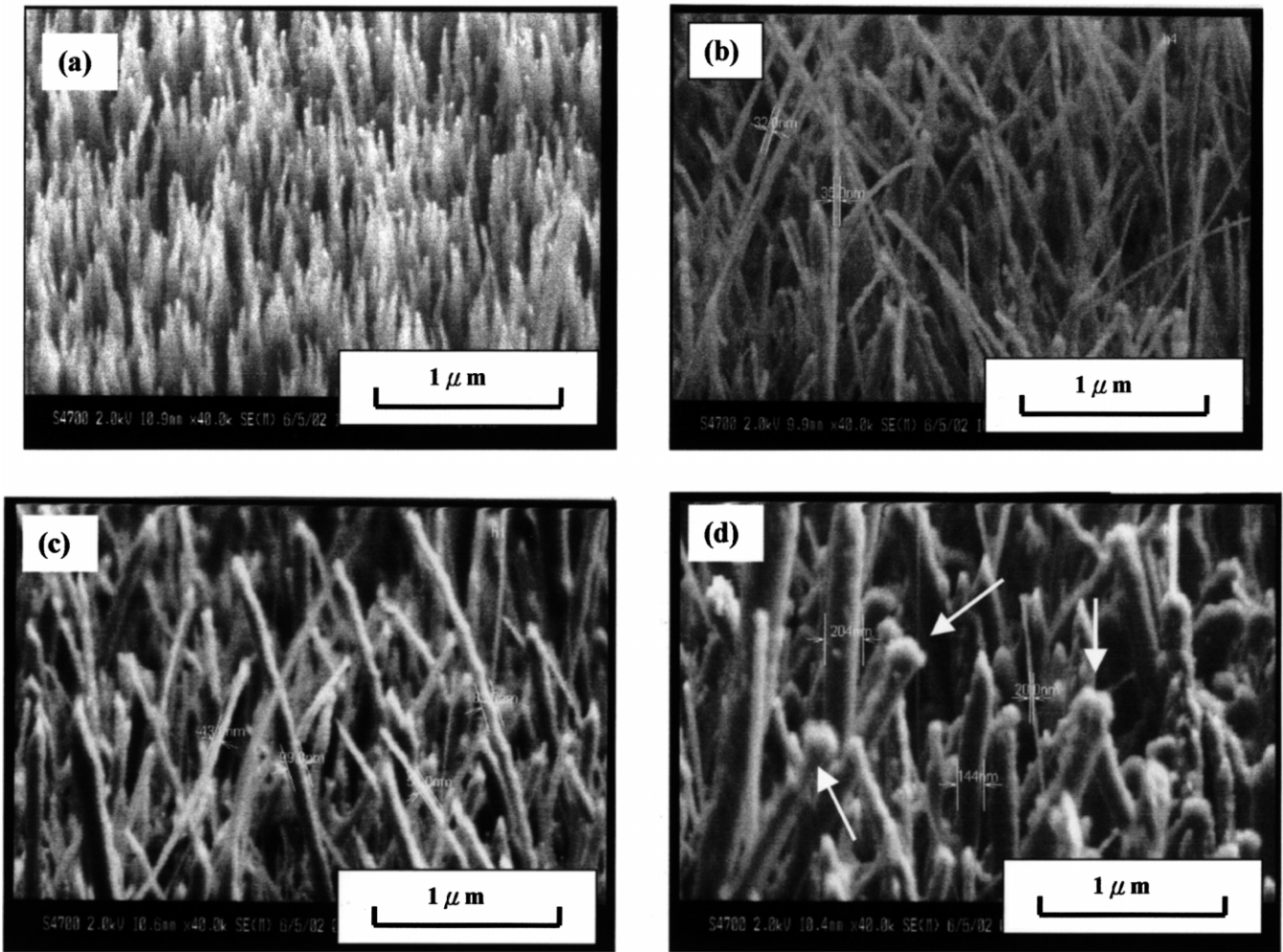


Fig. 3. SEM morphology image of vertically aligned CNT growth on an Fe-deposited substrate. (a) SEM image without H₂ plasma pretreatment. (b) Pretreated with H₂ plasma for 3 min. (c) Pretreated with H₂ plasma for 7 min. (d) Pretreated with H₂ plasma for 15 min.

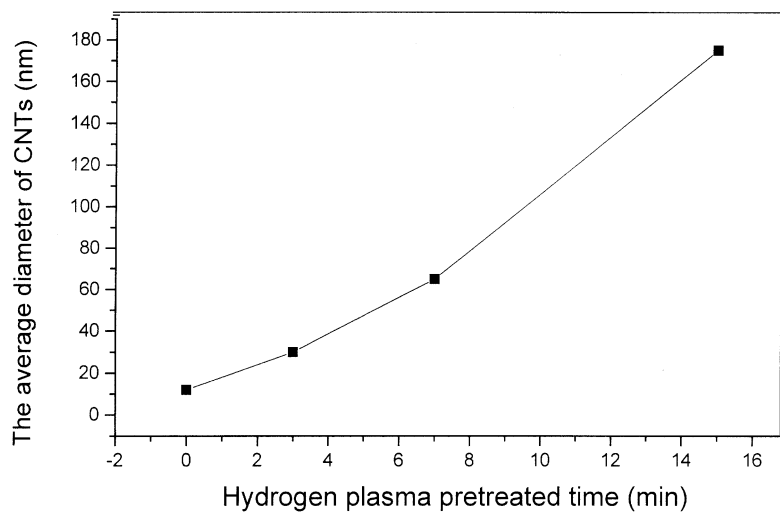


Fig. 4. The relation between diameter of CNTs and the H₂ plasma pretreatment time.

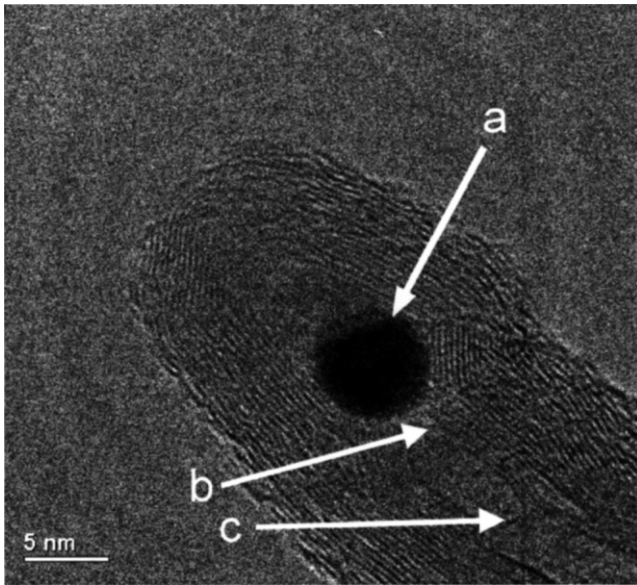


Fig. 5. HRTEM image for the multi-walled structure of sample A1.

unable to diffuse. The wall of CNTs was formed and rolled up in spherical and cylindrical shapes, and then hollow CNTs grow under the induction of Fe particle. CNTs are induced by DC bias to grow vertically.

(d) Carbon species were continuously supplied and diffused into the growing CNTs. The CNTs in the lateral direction with multi-walled structure occur due to the additive precipitation of carbon species, with mutual reaction of hydrogen and oxygen, resulting in multi-

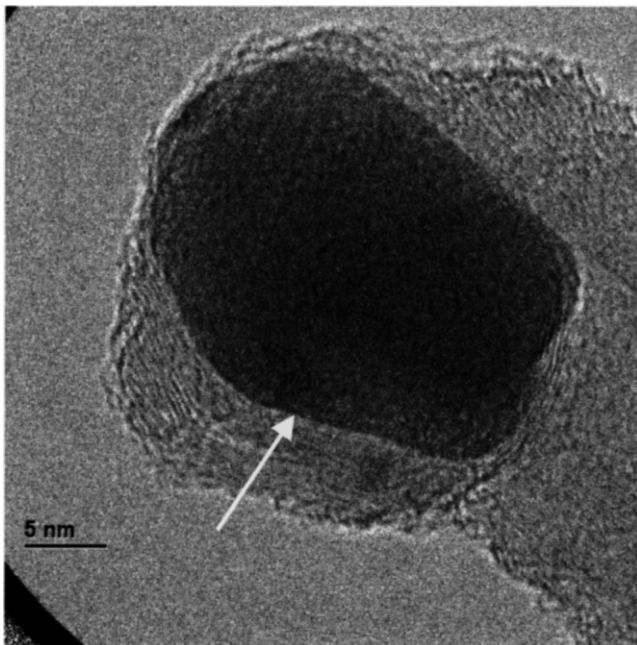


Fig. 6. HRTEM image for the multi-walled structure of sample A2.

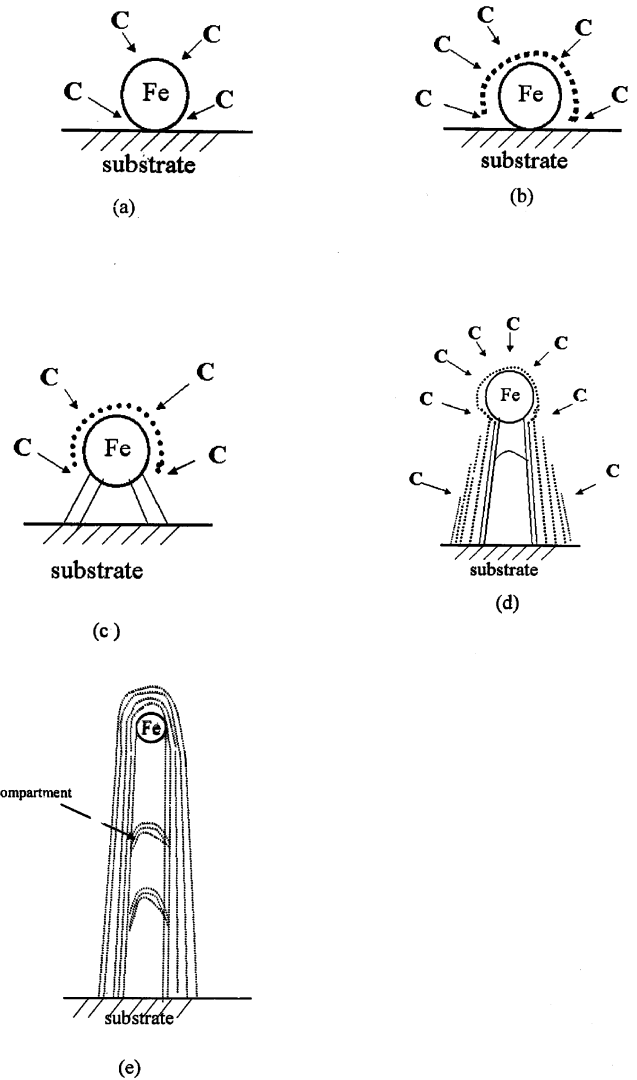


Fig. 7. Growth model of multi-walled CNTs.

walled CNTs. Carbon generated from the decomposition of CH_4 and CO_2 surrounds the outer tube wall and keeps on growing in the direction of catalysts due to the continuous carbon supply, forming multi-layer tube walls.

(e) Settlement of the deposited graphite on the inner tube walls induced by catalysts in the axial direction is graduated.

4. Conclusions

In summary, the MPCVD technique was adopted to grow aligned CNTs on Fe-deposited silicon substrates using CH_4 – CO_2 gas mixture. Fe particles cohered after H_2 plasma pretreatment, leading to a broader size distribution. The Fe particle changed from approximately spherical to the elliptic, further elongating to elliptic shapes in non-uniform size. The diameter of CNTs was

approximately 15 nm, made without H₂ plasma pretreatment, and 25–35, 40–90 and 200–300 nm for those pretreated with H₂ plasma for 3, 7 and 15 min, respectively. Hence, it can be concluded that the diameter of CNTs is controlled by the metal catalyst particle size in chemical vapor deposition growth. On the other hand, a significant difference in morphology in the carbon deposition was observed between Fe and Ti catalysts. By adjusting the growth parameters of CH₄ to CO₂, a high yield of vertically aligned CNTs was achieved for Fe-deposited substrates, but Ti was found to be not suitable as a catalyst in CNT production. Accordingly, on the basis of the experimental results, a possible growth model of multi-walled CNTs on Fe-deposited substrate was proposed.

Acknowledgments

The authors thank the National Science Council of Republic of China, Taiwan, for supporting this research under contract No. NSC89-2216-E-009-042. Technical support from the Semiconductor Research Center of National Chiao Tung University and National Nano Device Laboratory of NSC are also acknowledged.

References

- [1] S. Iijima, *Nature* 354 (1991) 56.
- [2] R. Stevens, C. Nguyen, A. Cassell, L. Delzeit, M. Meyyappan, J. Han, *Appl. Phys. Lett.* 77 (2000) 3453.
- [3] X.K. Wang, X.W. Lin, V.P. Dravid, J.B. Ketterson, R.P.H. Chang, *Appl. Phys. Lett.* 66 (1995) 2430.
- [4] L.C. Qin, D. Zhou, A.R. Krauss, D.M. Gruen, *Appl. Phys. Lett.* 72 (1998) 3437.
- [5] Z. Shi, Y. Lian, X. Zhou, et al., *Carbon* 37 (1999) 1449.
- [6] Z.P. Huang, J.W. Xu, Z.F. Ren, J.H. Wang, M.P. Siega, P.N. Provencio, *Appl. Phys. Lett.* 73 (1998) 3845.
- [7] C.J. Lee, J. Park, *Carbon* 39 (2001) 1891.
- [8] H.J. Dai, A.G. Rinzler, P. Nikolaev, A. Thess, D.T. Colbert, R.E. Smalley, *Chem. Phys. Lett.* 260 (1996) 471.
- [9] A. Fonseca, K. Hernadi, P. Piedigrosso, et al., *Electrochem. Soc.* 97 (1997) 884.
- [10] C.J. Lee, J. Park, Y. Huh, J.Y. Lee, *Chem. Phys. Lett.* 343 (2001) 33.
- [11] N.M. Rodriguez, *J. Mater. Res.* 8 (1993) 3233.
- [12] M.J. Yacaman, M.M. Yoshida, L. Rendon, J.G. Santiesteban, *Appl. Phys. Lett.* 62 (1993) 657.
- [13] E.F. Kukovitsky, S.G. L'vov, N.A. Sainov, V.A. Shustov, L.A. Chernozatonskii, *Chem. Phys. Lett.* 355 (2002) 497.
- [14] A.M. Benito, Y. Maniette, E. Munoz, M.T. Martinez, *Carbon* 36 (1998) 681.
- [15] A. Zhang, C. Li, S. Bao, Q. Xu, *Micro. Mesoporous Mater.* 29 (1999) 383.
- [16] M. Jung, K.Y. Eun, Y.I. Baik, K.R. Lee, J.K. Shin, S.T. Kim, *Thin Solid Films* 398 (2001) 150.
- [17] M. Chen, C.M. Chen, C.F. Chen, *J. Mater. Sci.* 37 (2002) 3561.
- [18] M. Chen, C.M. Chen, C.F. Chen, *Thin Solid Films* 420–421C (2002) 230.
- [19] M. Chen, C.M. Chen, S.C. Shi, C.F. Chen, *Jap. J. Appl. Phys.* 42 (2002) 614.
- [20] Y.C. Choi, Y.M. Shin, Y.H. Lee, et al., *Appl. Phys. Lett.* 76 (2000) 2367.
- [21] C.J. Lee, J. Park, *Appl. Phys. Lett.* 77 (21) (2000) 3397.
- [22] Y. Saito, T.J. Yoshikawa, *Cryst. Growth* 71 (1993) 154.
- [23] M. Jung, K.Y. Eun, J.K. Lee, Y.J. Baik, K.R. Lee, J.W. Park, *Diamond Relat. Mater.* 10 (2001) 1235.